Multi-vehicle Cooperative Control for Load Transportation ⋆

Tiago Valentim * **Rita Cunha** * **Paulo Oliveira** **
David Cabecinhas *,*** **Carlos Silvestre** *,***

* *Department of Electrical and Computer Engineering, Instituto Superior Técnico, Universidade de Lisboa, Portugal*
** *Department of Mechanical Engineering, Instituto Superior Técnico, Universidade de Lisboa, Portugal*
*** *Faculty of Science and Technology, University of Macau, Macau, China*

Abstract: This work proposes a cooperative control solution to the problem of transporting a suspended load using multiple quadrotor vehicles. The problem is addressed for two quadrotors, with a methodology that can be generalized for any number of quadrotors. A dynamic model of the system is developed considering a point-mass load, rigid massless cables, and neglecting aerodynamic effects of the cables. The concept of differential flatness is explored and a new set of flat outputs, which can be used to fully characterize the state of the system, is proposed. A nonlinear Lyapunov-based controller in cascaded form is derived, by defining adequate mappings between the cable tension vectors and the quadrotor thrust vectors and exploring the analogy with the problem of controlling a single quadrotor. Simulation results are presented for tracking of load trajectories. Comparisons are made with a free-flying quadrotor control scheme to highlight the enhanced performance of the proposed scheme.

Keywords: nonlinear control, differential flatness, cascaded systems, autonomous vehicles, slung-load transportation

1. INTRODUCTION

In recent years, there has been a rise in the use of Unmanned Aerial Vehicles (UAVs) for various applications. In particular, quadrotor UAVs have received a lot of attention due to their high maneuverability in 3D environments, high thrust to weight ratio and reduced mechanical complexity. Applications include coverage of media events (photography and filming), infrastructure inspections, and mobile sensor networks, to name a few. Among these applications, load transportation is a topic that has been explored for several years. As highlighted in Villa et al. (2018), it has gained importance in both civilian and military applications, taking advantage of the vehicles ability to describe precise trajectories for transportation of fragile cargo.

Research on slung-load transportation goes from path-planning to control system design and estimation problems. Several results available in the literature use the concept of differential flatness, which defines a class of dynamical systems for which all states and inputs can be described as functions of the so-called flat output and its time derivatives. This property has been explored to address both motion planning and tracking control problems. For example, the work in Sreenath et al. (2013) shows that a system comprised of a single quadrotor and a load connected by a inelastic massless cable is differentially flat and extends also the definition for the full hybrid system that results from considering the case when the cable is not taut. This concept is further developed in Sreenath and Kumar (2013), considering a rigid body load and proving differential flatness for 3 or more quadrotors. The work in Kotaru et al. (2017) develops further from Sreenath and Kumar (2013) by describing the cable via a mass-spring model to account for its elasticity. Although the resulting system is not differentially flat, a geometric controller is proposed and convergence is proven for the reduced dynamics via single perturbation theory. In Cabecinhas et al. (2019), a nonlinear Lyapunov-based trajectory tracking controller is proposed for the case of a single quadrotor and suspended load, which relies on expressing the system in an adequate form for application of the backstepping technique, providing asymptotic stabilization with a large region of attraction. The work in Lee et al. (2013) applies geometric control to address the problem of slung-load transportation using an arbitrary number of quadrotors and a point-mass load, proposing an inner-outer loop control structure.In Lee (2018) this control method is extended to consider a rigid-body load. Pereira et al. (2016) analyse the full model of a single quadrotor and a load and define the domains for the inputs and angular velocity of the cable where the cables remain taut and the quadrotor's thrust points outwards to avoid compression forces on the cables. In Pereira and Dimarogonas (2017) the problem of

⋆ This work was partially supported by the projects MYRG2018-00198-FST of the University of Macau; by the Macau Science and Technology, Development Fund under Grant FDCT/026/2017/A1 by Fundao para a Cincia e a Tecnologia (FCT) through the projects UID/EEA/50009/2019, LOTUS - PTDC/EEIAUT/ 5048/2014, HARMONY - PTDC/EEI-AUT/31411/2017.

controlling two drones with a slung-load is addressed by separating the problem into three decoupled systems and controlling each one separately: one for position, another for the yaw angles and a final one for the plane defined by the two cables.

In this work, we propose a cooperative control scheme for multi-vehicle load transportation, exploring the definition of a new set of flat outputs. These include the position of the load and a set of angles that completely define the cable directions and consequently the relative positions of the quadrotors. Explicit mappings between the cable tension vectors and the quadrotor thrust vectors are then explored to define an error system, starting with the load position error, progressing to the cable direction errors, and ending with quadrotors' thrust direction error. The resulting closed-loop system takes the form of a cascaded system, whose origin is shown to be asymptotically stable.

The paper is organized as follows. In Section 2, the model of the system to be adopted and the problem to be solved are introduced. In Section 3, the system is analyzed for differential flatness and the control scheme is derived. Simulation results are presented in Section 4 and Section 5 summarizes the contents of the paper.

2. PROBLEM STATEMENT

Consider two quadrotors, with masses m_{Q_1} and m_{Q_2}, connected by massless, rigid links with lengths l_1 and l_2 to a point-mass load with mass m_l. An inertial reference frame $\{I\}$ is introduced, along with two body reference frames $\{B_i\}$ where $i \in \{1, 2\}$, each one fixed to the center of mass of quadrotor i. The inertial reference frame has its z axis pointing downwards, in the direction of the gravity vector, which is assumed to be constant. As shown in Fig. 1, let the direction of each cable i be described by a unit vector $\boldsymbol{q}_i \in \mathbb{S}^2$, where $\mathbb{S}^2 = \{\boldsymbol{q}_i \in \mathbb{R}^3 \mid \|\boldsymbol{q}_i)\| = 1\}$, expressed in the inertial reference frame and centered at the origin of the body frame $\{B_i\}$. The load position expressed in $\{I\}$ is defined as $\boldsymbol{x}_l$ and the orientation of quadrotor i, or more specifically, the rotation matrix from $\{B_i\}$ to $\{I\}$ is defined as $R_{Q_i} \in \mathbb{SO}(3)$, where $\mathbb{SO}(3) = \{RR^T = I \mid det(R) = I\}$ denotes the Special Orthogonal Group of order 3.

Within this setting, the control objective consists of designing a control law to achieve tracking of a desired trajectory for the load, i.e. guarantee that the load position $\boldsymbol{x}_l(t)$ converges asymtptotically to $\boldsymbol{x}_{l_d}(t)$.

Given the rigid link assumption, it immediately follows that

$$\boldsymbol{x}_{Q_i} = \boldsymbol{x}_l - l_i \boldsymbol{q}_i \quad , \tag{1}$$

where $\boldsymbol{x}_{Q_i}$ is the position of quadrotor i expressed in $\{I\}$ (see Fig. 1). By Newton's Law, the following expression can be obtained for the total accelerations of the load and quadrotors

$$\begin{cases} m_l \ddot{\boldsymbol{x}}_l = -T_1 \boldsymbol{q}_1 - T_2 \boldsymbol{q}_2 + m_l g \boldsymbol{e}_3 = -T_{L_t} \boldsymbol{q}_t + m_l g \boldsymbol{e}_3 \\ m_{Q_i} \ddot{\boldsymbol{x}}_{Q_i} = T_i \boldsymbol{q}_i - T_{Q_i} \boldsymbol{r}_{Q_i} + m_{Q_i} g \boldsymbol{e}_3 \end{cases} \tag{2}$$

where $\ddot{\boldsymbol{x}}_l$ denotes the load linear acceleration, $\ddot{\boldsymbol{x}}_{Q_i}$ the acceleration of quadrotor i, g the gravitational acceleration, T_i the tension applied by link i, T_{Q_i} the thrust applied by quadrotor i, and $\boldsymbol{r}_{Q_i}$ the direction of that thrust, which coincides with the z-axis of the vehicle. The scalar T_{L_t} and unit vector $\boldsymbol{q}_t \in \mathbb{S}^2$ define the total tension norm and direction, respectively, and are such that $T_{L_t} \boldsymbol{q}_t = T_1 \boldsymbol{q}_1 + T_2 \boldsymbol{q}_2$.

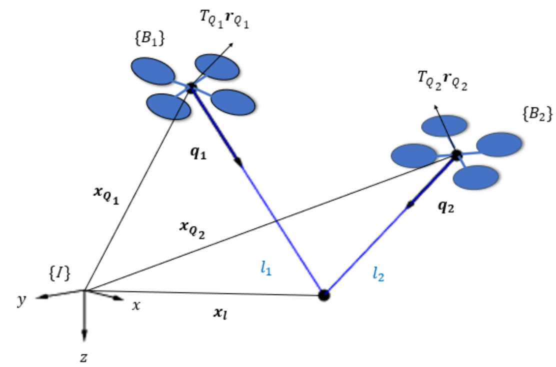

Fig. 1. Illustration of the problem statement (n = 2)

For the sake of simplicity, we assume that, for each quadrotor, an inner loop controller provides tracking of angular velocity commands and consider only the kinematics of $\boldsymbol{r}_{Q_i}$, assuming that the extra angular degree of freedom is independently controlled.

Using (1) and (2) similarly to Lee et al. (2013), and performing additional algebraic manipulations, the complete model can be written as

$$\begin{cases} \dot{\boldsymbol{x}}_l = \boldsymbol{v}_l \\ \dot{\boldsymbol{v}}_l = g\boldsymbol{e}_3 - M_q^{-1} \sum_{i=1}^{n} \alpha_i \boldsymbol{q}_i \\ \ddot{\boldsymbol{q}}_i = -\|\dot{\boldsymbol{q}}_i\|^2 \boldsymbol{q}_i + \frac{1}{l_i} \Pi_{q_i} \left(\frac{1}{m_{Q_i}} T_{Q_i} \boldsymbol{r}_{Q_i} - M_q^{-1} \sum_{j=1}^{n} \alpha_j \boldsymbol{q}_j \right) \\ \dot{\boldsymbol{r}}_{Q_i} = \boldsymbol{u}_{Q_i} \end{cases} \tag{3}$$

where the following variables are introduced

- $\boldsymbol{v}_l$ is the velocity of the load;
- M_q is the positive definite symmetric matrix given by $M_q = m_l I + \sum_{i=1}^{n} m_{Q_i} \boldsymbol{q}_i \boldsymbol{q}_i^T$
- α_i is an auxiliary variable given by $\alpha_i = \boldsymbol{q}_i^T T_{Q_i} \boldsymbol{r}_{Q_i} + m_{Q_i} l_i \|\dot{\boldsymbol{q}}_i\|^2$
- $\boldsymbol{u}_{Q_i}$ is the simplified quadrotor angular velocity input, which satisfies $\boldsymbol{r}_{Q_i}^T \boldsymbol{u}_{Q_i} = 0$.

One aspect to consider when analysing the model equations is the fact for each quadrotor only the thrust component that is parallel to the respective links $\boldsymbol{q}_i^T T_{Q_i} \boldsymbol{r}_{Q_i}$ has an effect on the dynamics of the load, whereas the perpendicular component of the thrust $\Pi_{\boldsymbol{q}_i} T_{Q_i} \boldsymbol{r}_{Q_i}$ can be used to control the direction of cable i. This already gives insight to the control strategy that will be developed in the following sections.

3. DESIGN OF THE TRACKING CONTROLLER FOR LOAD TRANSPORTATION

3.1 Differential flatness property

A system is said to be differentially flat if there exists a set of outputs such that all states and inputs can be expressed as functions of that output and its time derivatives. As pointed out in the introduction, other authors have tackled the load transportation problem by defining a set of flat outputs for the system. For the particular case of a point-mass model and n quadrotors, the system is differentially flat, with flat outputs given by the yaw angles of the quadrotors ψ_i, the position of the load $\boldsymbol{x}_l$ and the values of $n-1$ tension vectors $T_i\boldsymbol{q}_i$.

In this section an alternative set of flat ouputs is proposed, from which the flat outputs described previously can be reached. The problem is defined for the case of a point mass load and two quadrotors. Figure 2 displays the problem configuration, introducing the angles β_1, β_2, and γ, which define the orientation of $\boldsymbol{q}_1$ and $\boldsymbol{q}_2$ relative $\boldsymbol{q}_t$ and satisfy

$$\begin{cases} \beta_1 = arcos(\boldsymbol{q}_t \cdot \boldsymbol{q}_1), & \beta_1 \in [0,\pi] \\ \beta_2 = arcos(\boldsymbol{q}_t \cdot \boldsymbol{q}_2), & \beta_2 \in [0,\pi] \\ \gamma = asin(-\dfrac{\boldsymbol{q}_2 \times \boldsymbol{q}_1}{\|\boldsymbol{q}_2 \times \boldsymbol{q}_1\|} \cdot \boldsymbol{e}'_y), & \gamma \in [0, 2\pi[, \end{cases}$$

where $\boldsymbol{q}_t$ is total tension direction introduced in (2). Given $\boldsymbol{q}_t$, β_1, β_2, and γ, the tension directions $\boldsymbol{q}_1$ and $\boldsymbol{q}_2$ can be specified as

$$\boldsymbol{q}_i = R_{aux}R_x(\gamma)R_z((-1)^{i-1}\beta_i)\boldsymbol{e}_1, \tag{4}$$

where

$$R_{aux} = R_y(\phi_t)R_z(\theta_t)$$

and

$$\begin{cases} \phi_t = arcos(\dfrac{T_{L_t} \cdot \boldsymbol{e}_x}{\|T_{L_{zx}}\|}), & 0 < \phi_t \le \pi \\ \\ \phi_t = 2\pi - arcos(\dfrac{T_{L_t} \cdot \boldsymbol{e}_x}{\|T_{L_{zx}}\|}), & \pi < \phi_t \le 2\pi, \\ \quad with \quad T_{L_{zx}} = [T_{L_t} \cdot \boldsymbol{e}_1 \ 0 \ T_{L_t} \cdot \boldsymbol{e}_3]\boldsymbol{q}_t \end{cases}$$

and $\theta_t = \frac{\pi}{2} - arcos(\frac{T_{L_t} \cdot \boldsymbol{e}_y}{\|T_{L_t}\boldsymbol{q}_t\|}) \in [0,\pi]$. The rotation matrix R_{aux} defines the orientation of an auxiliary reference frame with x-axis aligned with $\boldsymbol{q}_t$ relative to the inertial frame.

Assumption 1. $T_{L_t}\boldsymbol{q}_t$ is always non-zero and the third component is always non-zero, with each cable always being taut, i.e, $T_{Li} \neq 0$.

This assumption guarantees that the plane formed by $\boldsymbol{q}_1$ and $\boldsymbol{q}_2$ (which also contains $\boldsymbol{q}_t$) is always well-defined and a mapping for the thrust values of each quadrotor is guaranteed to exist.

Theorem 2. Under assumption 1, the system presented in (3) is differentially flat, with the set of flat outputs given by $\boldsymbol{x}_l$, ψ_1, ψ_2, β_1, β_2 and γ.

Proof 1. By use of (2), given a desired trajectory for the load $\boldsymbol{x}_l$ and respective acceleration $\ddot{\boldsymbol{x}}_l$, we can calculate a desired Tension vector $T_{L_t}\boldsymbol{q}_t$.

Given β_1, β_2, and γ, the directions $\boldsymbol{q}_1$ and $\boldsymbol{q}_2$ can be immediately recovered from (4). To recover T_1 and T_2 we note that $T_1\boldsymbol{q}_1 + T_2\boldsymbol{q}_2 = T_{L_t}\boldsymbol{q}_t$. It follows that

$$R_{aux}R_x(\gamma)(T_1R_y(\beta_1) + T_2R_y(-\beta_2))\boldsymbol{e}_1 = T_t\boldsymbol{q}_t,$$

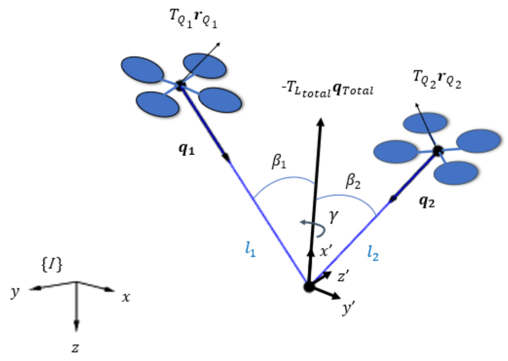

Fig. 2. Flat outputs Illustration (n = 2)

yielding

$$\begin{bmatrix} cos(\beta_1) & cos(\beta_2) \\ sin(\beta_1) & -sin(\beta_2) \end{bmatrix} \begin{bmatrix} T_{L_1} \\ T_{L_2} \end{bmatrix} = \begin{bmatrix} T_{L_t} \\ 0 \end{bmatrix} \tag{5}$$

Thus, from $\ddot{\boldsymbol{x}}_l$, β_1, β_2, and γ the tension of either one of the cables can be determined, which together with the yaw angles of the quadrotors ψ_1 and ψ_2 form the outputs that are shown to be flat in Sreenath and Kumar (2013).

Notice that the transformation is only well defined if the matrix in (5) is invertible. This is the case if β_1 and β_2 $\in (0,\ \frac{\pi}{2})$ rad, which defines a physically meaningful range for these angles.

3.2 Outer loop control scheme

In this section, the control formulation will be given for the configuration presented in 2. An analogy to a free flying quadrotor control formulation will be made, following an approach similar to the one in Cabecinhas et al. (2019) for the case of a single quadrotor with suspended load, but now extended to the case of two vehicles. To simplify the controller design and follow a constructive approach, a simplified model that neglects the orientation dynamics of both quadrotors is chosen as a starting point, meaning that $T_{Q_i}\boldsymbol{r}_{Q_i}$ can be set instantaneously and used as inputs. Under this assumption, a parallel with the dynamics for a free flying quadrotor can be drawn by applying an adequate change of variables.

Considering the definition of the total tension vector given in (2) and new variables τ_1 and τ_2 that satisfy $\boldsymbol{\tau}_i = \frac{1}{l_i}\Pi_{q_i}(\frac{1}{m_{Q_i}}T_{Q_i}\boldsymbol{r}_{Q_i} - M_q^{-1}\sum_j \alpha_j\boldsymbol{q}_j)$, the overall system dynamics described in (3) can be rewritten as

$$\begin{cases} \ddot{\boldsymbol{x}}_l = -\dfrac{1}{m_l}(T_1\boldsymbol{q}_1 + T_2\boldsymbol{q}_2) + g\boldsymbol{e}_3 \\ \ddot{\boldsymbol{q}}_i = -\|\dot{\boldsymbol{q}}_i\|^2\boldsymbol{q}_i + \Pi_{q_i}\boldsymbol{\tau}_i \end{cases} \tag{6}$$

which highlights the similarity with the free flying quadrotor system described by

$$\begin{cases} \ddot{\boldsymbol{x}} = -T\boldsymbol{r} + g\boldsymbol{e}_3 \\ \ddot{\boldsymbol{r}} = -\|\dot{\boldsymbol{r}}\|^2\mathbf{r} + \Pi_r\boldsymbol{\tau} \end{cases} \tag{7}$$

Using $(T_1, T_2, \boldsymbol{\tau}_1, \boldsymbol{\tau}_2)$ as virtual inputs $(T_1^*, T_2^*, \boldsymbol{\tau}_1^*, \boldsymbol{\tau}_2^*)$, a trajectory tracking controller can be defined for (6), much in the same way as for (7) with inputs given by $(T, \boldsymbol{\tau})$. To this end, the following assumption needs to be satisfied, to guarantee that all variables and respective time-derivates used to define the control laws are well-defined.

Assumption 3. The desired trajectories $\boldsymbol{x}_{ld}$ are class C^5 functions of time, with bounded time derivatives.

To further detail this strategy, consider the tracking errors $\tilde{\boldsymbol{x}}_l = \boldsymbol{x}_l - \boldsymbol{x}_{ld}$ and $\tilde{\boldsymbol{v}}_l = \boldsymbol{v}_l - \dot{\boldsymbol{x}}_{ld}$ and the PD-like controller $\boldsymbol{a}_{ld} = g\boldsymbol{e}_3 - \ddot{\boldsymbol{x}}_{ld} + k_x\tilde{\boldsymbol{x}}_l + k_v\tilde{\boldsymbol{v}}_l$. Then, the desired tensions T_{1d} and T_{2d} and desired tension directions $\boldsymbol{q}_{1d}$ and $\boldsymbol{q}_{2d}$ can be computed via (4) and (5) with $T_{L_t}\boldsymbol{q}_t = m_l\boldsymbol{a}_{ld}$. Defining

$$T_i^* = \boldsymbol{q}_i^T T_{id}\boldsymbol{q}_{id}, \tag{8}$$

the closed-loop linear dynamics can be written as

$$\begin{cases} \dot{\tilde{\boldsymbol{x}}}_l = \tilde{\boldsymbol{v}}_l \\ \dot{\tilde{\boldsymbol{v}}}_l = -k_x\tilde{\boldsymbol{x}}_l - k_v\tilde{\boldsymbol{v}}_l - \dfrac{T_{1d}}{m_l}\Pi_{q_1}\tilde{\boldsymbol{q}}_1 - \dfrac{T_{2d}}{m_l}\Pi_{q_2}\tilde{\boldsymbol{q}}_2 \end{cases} \tag{9}$$

where $\tilde{\boldsymbol{q}}_i = \boldsymbol{q}_i - \boldsymbol{q}_{id}$ gives the error between current and desired orientations. The mismatch between $\boldsymbol{q}_i$ and $\boldsymbol{q}_{id}$ can then be driven to zero by again defining PD controllers for the inputs τ_i^*, taking into account the fact that now the state $\boldsymbol{q}_i$ evolves on the two-sphere $\mathbb{S}(2)$. Defining the angular velocity errors as $\tilde{\boldsymbol{\omega}}_i = \dot{\boldsymbol{q}}_i + S(\boldsymbol{q}_i)S(\boldsymbol{q}_{id})\dot{\boldsymbol{q}}_{id}$ and using

$$\begin{aligned} \boldsymbol{\tau}_i^* = &-\Pi_{q_i}(k_q\tilde{\boldsymbol{q}}_i + k_\omega\tilde{\boldsymbol{\omega}}_i) \\ &- S(\boldsymbol{q}_i)(S(\boldsymbol{q}_{id})\ddot{\boldsymbol{q}}_{id} - \dot{\boldsymbol{q}}_i\boldsymbol{q}_i^T S(\boldsymbol{q}_{id})\dot{\boldsymbol{q}}_{id}) \end{aligned} \tag{10}$$

the closed-loop dynamics for the system with state $(\tilde{\boldsymbol{q}}_i, \tilde{\boldsymbol{\omega}}_i)$ can be written as

$$\begin{cases} \dot{\tilde{\boldsymbol{q}}}_i = -S(\tilde{\boldsymbol{q}}_i)S(\boldsymbol{q}_{id})\dot{\boldsymbol{q}}_{id} + \tilde{\boldsymbol{\omega}}_i \\ \dot{\tilde{\boldsymbol{\omega}}}_i = \boldsymbol{q}_i(\dot{\boldsymbol{q}}_i^T\tilde{\boldsymbol{\omega}}_i - \|\dot{\boldsymbol{q}}_i\|^2) - \Pi_{q_i}(k_q\tilde{\boldsymbol{q}}_i + k_\omega\tilde{\boldsymbol{\omega}}_i) \end{cases} \tag{11}$$

We can then show that $(\tilde{\boldsymbol{q}}_i, \tilde{\boldsymbol{\omega}}_i)$ converges to zero, and consequently all tracking errors also converge to zero. The following theorem summarizes these results.

Theorem 4. Let the thrust inputs (T_1^*, T_2^*) be given by (8) and the torque inputs $(\boldsymbol{\tau}_1^*, \boldsymbol{\tau}_2^*)$ be given by (10). Then, the origin of the closed-loop system described by (9) and (11), with state $(\tilde{\boldsymbol{x}}_l, \tilde{\boldsymbol{v}}_l, \tilde{\boldsymbol{q}}_1, \tilde{\boldsymbol{\omega}}_1, \tilde{\boldsymbol{q}}_2, \tilde{\boldsymbol{\omega}}_2)$ is uniformly asymptotically stable.

Proof 2. We start by showing that the origin of (11) is asymptotically stable. Considering the Lyapunov function $V_q = \frac{k_q}{2}\|\tilde{\boldsymbol{q}}_i\|^2 + \frac{1}{2}\|\tilde{\boldsymbol{\omega}}_i\|^2$ and taking the time-derivative along the trajectories of the system, we obtain $\dot{V}_q = -k_\omega\|\tilde{\boldsymbol{\omega}}_i\|^2 \leq 0$, which implies that V_q is non-increasing, all states are bounded, and the origin of (11) is uniformly stable. By showing that all states and consequently $\dot{V}_q$ are uniformly continuous and resorting to Barbalat's Lemma, we can also conclude that $\tilde{\boldsymbol{\omega}}_i$ converges to zero and $\boldsymbol{q}_i$ converges to either $\boldsymbol{q}_{id}$ or $-\boldsymbol{q}_{id}$. Additional arguments based on linearization show that the equilibrium point $-\boldsymbol{q}_{id}$ is unstable (see Lee (2016) for details). Considering now the linear dynamics (9) together with angular dynamics (11), $i \in \{1, 2\}$, we can rewrite the system in cascaded form as

$$\begin{cases} \dot{\eta} = f(\eta, \xi, t) \\ \dot{\xi} = g(\xi, t) \end{cases} \tag{12}$$

with $\eta = [\tilde{\boldsymbol{x}}_l^T \ \tilde{\boldsymbol{v}}_l^T]^T$ and $\xi = [\tilde{\boldsymbol{q}}_1^T \ \tilde{\boldsymbol{\omega}}_1^T \ \tilde{\boldsymbol{q}}_2^T \ \tilde{\boldsymbol{\omega}}_2^T]^T$. Given that the origin of $\dot{\eta} = f(\eta, 0, t)$ is globally exponentially stable (the system becomes autonomous) and the origin of $\dot{\xi} = g(\xi, t)$ is uniformly asymptotically stable, we can immediately conclude that in some bounded region all error states converge to zero and thus the origin of the full closed-loop system is uniformly asymptotically stable.

3.3 Mapping cable tensions to quadrotor thrust forces

The outer loop controller described in Section 3.2 considers the virtual inputs $(T_1^*,\boldsymbol{\tau}_1^*)$ and $(T_2^*,\boldsymbol{\tau}_2^*)$, which need to be mapped into the quadrotor virtual inputs $T_{Q_1}^*\boldsymbol{r}_{Q_1}^*$ and $T_{Q_2}^*\boldsymbol{r}_{Q_2}^*$, respectively. For convenience the superscript is dropped, given that the mapping applies not only to virtual but also to the real variables. To determine this mapping, $T_{Q_i}\boldsymbol{r}_{Q_i}$ are decomposed into two components, one parallel and the other perpendicular to $\boldsymbol{q}_i$, i.e.

$$T_{Q_i}\boldsymbol{r}_{Q_i} = u_i\boldsymbol{q}_i + \Pi_{\boldsymbol{q}_i}T_{Q_i}\boldsymbol{r}_{Q_i}, \tag{13}$$

where $u_i = \boldsymbol{q}_i^T T_{Q_i}\boldsymbol{r}_{Q_i}$.

Recalling that in (3) u_i appears in the equation for $\dot{\boldsymbol{v}}_l$, whereas $\Pi_{\boldsymbol{q}_i}$ appears in the equation for $\dot{\boldsymbol{\omega}}_i$ suggest the definition of two mappings. The first between (T_1,T_2) and (u_1,u_2) and the second between $(\boldsymbol{\tau}_1,\boldsymbol{\tau}_2)$ and $\Pi_{\boldsymbol{q}_i}T_{Q_i}\boldsymbol{r}_{Q_i}$.

Lemma 5. If the cables are not collinear, the mapping from the cable tensions (T_1,T_2) to the parallel components (u_1, u_2) is given by

$$u_1 = (1 + \frac{m_{Q_1}}{m_l})T_1 + \frac{m_{Q_1}}{m_l}\boldsymbol{q}_1^T\boldsymbol{q}_2 T_2 - m_{Q_1}l_1\|\dot{\boldsymbol{q}}_1\|^2 \tag{14}$$

$$u_2 = (1 + \frac{m_{Q_2}}{m_l})T_2 + \frac{m_{Q_2}}{m_l}\boldsymbol{q}_2^T\boldsymbol{q}_1 T_1 - m_{Q_2}l_2\|\dot{\boldsymbol{q}}_2\|^2. \tag{15}$$

Proof 3. From (2) and (3), we have that

$$M_q(T_1\boldsymbol{q}_1 + T_2\boldsymbol{q}_2) = m_l(\alpha_1\boldsymbol{q}_1 + \alpha_2\boldsymbol{q}_2),$$

where $\alpha_i = u_i + m_{Q_i}l_i\|\dot{\boldsymbol{q}}_i\|^2$. Rearranging the terms as linear combinations of $\boldsymbol{q}_1$ and $\boldsymbol{q}_2$, we obtain

$$\delta_1\boldsymbol{q}_1 + \delta_2\boldsymbol{q}_2 = 0 \tag{16}$$

with δ_1 and δ_2 given by

$$\begin{cases} \delta_1 = (m_l + m_{Q_1})T_1 + m_{Q_1}\boldsymbol{q}_1^T\boldsymbol{q}_2T_2 - m_l\alpha_1 \\ \delta_2 = (m_l + m_{Q_2})T_2 + m_{Q_2}\boldsymbol{q}_2^T\boldsymbol{q}_1T_1 - m_l\alpha_2 \end{cases} \tag{17}$$

If $\boldsymbol{q}_1$ and $\boldsymbol{q}_2$ are noncollinear then (16) only admits the trivial solution $\delta_1 = \delta_2 = 0$, yielding (14) and (15).

To obtain the second mapping note that, from (2) and the second time-derivative of (1), we can write

$$m_{Q_i}(\ddot{\boldsymbol{x}}_l - g\boldsymbol{e}_3 - l_i\ddot{\boldsymbol{q}}_i) = T_i\boldsymbol{q}_i - T_{Q_i}\boldsymbol{r}_{Q_i}. \tag{18}$$

It then follows from (6) that

$$\begin{cases} \Pi_{\boldsymbol{q}_1}T_{Q_1}\boldsymbol{r}_{Q_1} = m_{Q_1}\Pi_{\boldsymbol{q}_1}(l_1\boldsymbol{\tau}_1 + \dfrac{T_2}{m_l}\boldsymbol{q}_2) \\ \Pi_{\boldsymbol{q}_2}T_{Q_2}\boldsymbol{r}_{Q_2} = m_{Q_2}\Pi_{\boldsymbol{q}_2}(l_2\boldsymbol{\tau}_2 + \dfrac{T_1}{m_l}\boldsymbol{q}_1), \end{cases} \tag{19}$$

and thus each quadrotor thrust can be selected through the combined mapping (13).

3.4 Inner loop control

In the previous section, the outer loop control scheme was fully developed, under the assumption that the orientation dynamics is negligible, when compared to the position of the load and attitude control of the cables. This assumption is now lifted and the inner loop control scheme developed. First, the desired quadrotors thrusts $(T_{Q_i}^*, \boldsymbol{r}_{Q_i}^*)$ are defined as functions of the virtual tensions and torques $(T_i^*, \boldsymbol{\tau}_i^*)$. Second, a inner-loop orientation controller is designed to take $\boldsymbol{r}_{Q_i}$ to $\boldsymbol{r}_{Q_i}^*$, exploring once again the cascaded form of the system.

According to (13), the desired quadrotor thrust vectors take the form

$$
\begin{aligned}
T^*_{Q_i}\boldsymbol{r}^*_{Q_i} =& \boldsymbol{q}_i((1+\frac{m_{Q_i}}{m_l})T^*_i + \frac{m_{Q_i}}{m_l}\boldsymbol{q}_i^T T^*_j \boldsymbol{q}_j - m_{Q_i} l_i \|\dot{\boldsymbol{q}}_i\|^2) \\
&+ m_{Q_i}\Pi_{q_i}(l_i \boldsymbol{\tau}^*_i + \frac{1}{m_l}T^*_j \boldsymbol{q}_j) \qquad (20)
\end{aligned}
$$

with $(i,j) \in \{(1,2),(2,1)\}$. Note that (20) is defined as a function of the real values of $\boldsymbol{q}_1$ and $\boldsymbol{q}_2$, not the desired ones. Adding and subtracting $M_q^{-1}\sum_i \boldsymbol{q}_i\boldsymbol{q}_i^T T^*_{Q_i}\boldsymbol{r}^*_i$ and $\frac{1}{m_{Q_i}l_i}\Pi_{q_i}T^*_{Q_i}\boldsymbol{r}^*_{Q_i}$ to the linear and angular dynamics, respectively, and after some algebraic manipulations we can write

$$
\begin{aligned}
\dot{\boldsymbol{v}}_l =& g\boldsymbol{e}_3 - \sum_i \left(\frac{T^*_i}{m_l}\boldsymbol{q}_i + M_q^{-1}\boldsymbol{q}_i\boldsymbol{q}_i^T(T_{Q_i}\boldsymbol{r}_{Q_i} - T^*_{Q_i}\boldsymbol{r}^*_{Q_i})\right) \\
\ddot{\boldsymbol{q}}_i =& -\|\dot{\boldsymbol{q}}_i\|^2\boldsymbol{q}_i + \Pi_{q_i}\boldsymbol{\tau}^*_i \\
&- \frac{1}{l_i}\Pi_{q_i}M_q^{-1}\sum_j \boldsymbol{q}_j\boldsymbol{q}_j{}^T(T_{Q_j}\boldsymbol{r}_{Q_j} - T^*_{Q_j}\boldsymbol{r}^*_{Q_j}) \\
&+ \frac{1}{m_{Q_i}l_i}\Pi_{q_i}(T_{Q_i}\boldsymbol{r}_{Q_i} - T^*_{Q_i}\boldsymbol{r}^*_{Q_i})
\end{aligned}
$$

Finally, setting

$$
T_{Q_i} = T^*_{Q_i}\boldsymbol{r}^T_{Q_i}\boldsymbol{r}^*_{Q_i}, \qquad (21)
$$

introducing the new error variable $\tilde{\boldsymbol{r}}_{Q_i} = \boldsymbol{r}_{Q_i} - \boldsymbol{r}^*_{Q_i}$, and transforming into the error system, the full error system can be described by

$$
\begin{cases}
\dot{\tilde{\boldsymbol{x}}}_l = \tilde{\boldsymbol{v}}_l \\
\dot{\tilde{\boldsymbol{v}}}_l = -k_x\tilde{\boldsymbol{x}}_l - k_v\tilde{\boldsymbol{v}}_l - \frac{T_{1d}}{m_l}\Pi_{q_1}\tilde{\boldsymbol{q}}_1 - \frac{T_{2d}}{m_l}\Pi_{q_2}\tilde{\boldsymbol{q}}_2 \\
+M_q^{-1}\sum_i \boldsymbol{q}_i\boldsymbol{q}_i^T\Pi_{\boldsymbol{r}_{Q_i}}T^*_{Q_i}\tilde{\boldsymbol{r}}_{Q_i}
\end{cases} \qquad (22)
$$

and

$$
\begin{cases}
\dot{\tilde{\boldsymbol{q}}}_i = -S(\tilde{\boldsymbol{q}}_i)S(\boldsymbol{q}_{id})\dot{\boldsymbol{q}}_{id} + \tilde{\boldsymbol{\omega}}_i \\
\dot{\tilde{\boldsymbol{\omega}}}_i = \boldsymbol{q}_i(\dot{\boldsymbol{q}}_i^T\tilde{\boldsymbol{\omega}}_i - \|\dot{\boldsymbol{q}}_i\|^2) - \Pi_{q_i}(k_q\tilde{\boldsymbol{q}}_i + k_\omega\tilde{\boldsymbol{\omega}}_i) \\
-\frac{1}{l_i}\Pi_{q_i}(M_q^{-1}\sum_j \boldsymbol{q}_j\boldsymbol{q}_j^T\Pi_{\boldsymbol{r}_{Q_j}}T^*_{Q_j}\tilde{\boldsymbol{r}}_{Q_j} + \frac{1}{m_{Q_i}}\Pi_{\boldsymbol{r}_{Q_i}}T^*_{Q_i}\tilde{\boldsymbol{r}}_{Q_i}) \\
\dot{\tilde{\boldsymbol{r}}}_{Q_i} = -S(\tilde{\boldsymbol{r}}_{Q_i})S(\boldsymbol{r}^*_{Q_i})\dot{\boldsymbol{r}}^*_{Q_i} + \dot{\boldsymbol{r}}_{Q_i} + S(\boldsymbol{r}_{Q_i})S(\boldsymbol{r}^*_{Q_i})\dot{\boldsymbol{r}}^*_{Q_i}
\end{cases} \qquad (23)
$$

Again, the system takes a cascaded form and the convergence of $\tilde{\boldsymbol{r}}_{Q_i}$ to zero guarantees that there exists a neighborhood of the origin inside which all error states converge to zero.

Theorem 6. Let the quadrotor thrust inputs (T_{Q_1}, T_{Q_2}) be given by (21) and the angular rate inputs $(\dot{\boldsymbol{r}}_{Q_1}, \dot{\boldsymbol{r}}_{Q_2})$ be given by

$$
\begin{aligned}
\dot{\boldsymbol{r}}_{Q_i} =& -k_Q\Pi_{\boldsymbol{r}_{Q_i}}\tilde{\boldsymbol{r}}_{Q_i} - S(\boldsymbol{r}_{Q_i})S(\boldsymbol{r}^*_{Q_i})\dot{\boldsymbol{r}}^*_{Q_i} \\
&- \frac{T^*_{Q_i}}{l_i}\Pi_{\boldsymbol{r}_{Q_i}}(\frac{1}{m_{Q_i}}I + \boldsymbol{q}_i\boldsymbol{q}_i^T M_q^{-T})\tilde{\boldsymbol{\omega}}_i \qquad (24)
\end{aligned}
$$

Then, the origin of the closed-loop system described by (22) and (23), with state $(\tilde{\boldsymbol{x}}_l, \tilde{\boldsymbol{v}}_l, \tilde{\boldsymbol{q}}_1, \tilde{\boldsymbol{\omega}}_1, \tilde{\boldsymbol{q}}_2, \tilde{\boldsymbol{\omega}}_2, \tilde{\boldsymbol{r}}_{Q_1}, \tilde{\boldsymbol{r}}_{Q_2})$ is uniformly asymptotically stable.

Proof 4. Considering the system described by (23), the Lyapunov function

$$
W_i = \sum_i \left(\frac{k_q}{2}\|\tilde{\boldsymbol{q}}_i\|^2 + \frac{1}{2}\|\tilde{\boldsymbol{\omega}}_i\|^2 + \frac{1}{2}\|\tilde{\boldsymbol{r}}_i\|^2\right) \qquad (25)
$$

has negative semi-definite time derivative given by

$$
\dot{W}_i = -k_\omega\|\tilde{\boldsymbol{\omega}}_i\|^2 - k_Q\tilde{\boldsymbol{r}}^T_{Q_i}\Pi_{\boldsymbol{r}_{Q_i}}\tilde{\boldsymbol{r}}_{Q_i}. \qquad (26)
$$

Invoking once again Barbalat's Lemma, we can show that the origin of (23) is uniformly asymptotically stable. Finally, using the same cascaded form as in (12), but now with $\eta = [\tilde{\boldsymbol{x}}_l^T\ \tilde{\boldsymbol{v}}_l^T]^T$ and $\xi = [\tilde{\boldsymbol{q}}_1^T\ \tilde{\boldsymbol{\omega}}_1^T\ \tilde{\boldsymbol{q}}_2^T\ \tilde{\boldsymbol{\omega}}_2^T\ \tilde{\boldsymbol{r}}_{Q_1}^T\ \tilde{\boldsymbol{r}}_{Q_2}^T]^T$, we can again conclude that the origin of the full closed-loop system with state (η, ξ) is uniformly asymptotically stable.

4. RESULTS

In this section, simulation results are presented for a circular trajectory with fixed altitude. One term in the control law requires special attention: the time derivative of the desired orientation vector $\dot{\boldsymbol{r}}^*_{Q_i}$. This term will be computed numerically via the approximation with a band pass filter, which accurately represents this derivative for most trajectories. As presented next, for the selected gains K_{Q_1}, K_{Q_2} and factors L_1, L_2, this approximation is able to deliver adequate performance.

Three controllers were tested for the previous trajectories: the nonlinear Lyapunov based controller with no inner loop dynamics (assumed instantaneous), the nonlinear Lyapunov based controller with the inner loop controller proposed in this paper, and a free flying controller applied to both quadrotors. The free flying case was constructed by considering the desired load trajectory and reference angles β_i and γ and computing the corresponding nominal trajectories for each of the quadrotors. For control purposes, free flying quadrotor models were considered, neglecting the coupling forces due to the cable connections.The selected trajectory is given by

$$
\boldsymbol{x}_{ld}(t) = A\left[\sin(\omega t)\ \cos(\omega t)\ 0\right]^T,
$$

where $\omega = \frac{\pi}{2}$ rad/s. The initial position was selected to be at an offset of $[3, -2, 2]$ m from the initial desired position in the circular trajectory. The flat output angles β_1, β_2 and γ were kept constant at $\frac{\pi}{4}$, $\frac{\pi}{4}$, and 0 rad, respectively.

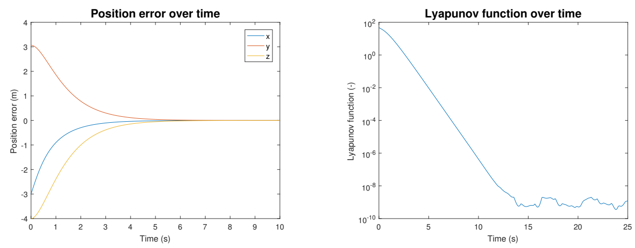

Fig. 3. Simulation results for the circular trajectory - no inner loop dynamics

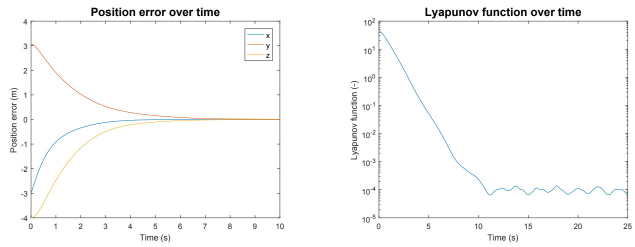

Fig. 4. Simulation results for the circular trajectory - full dynamics

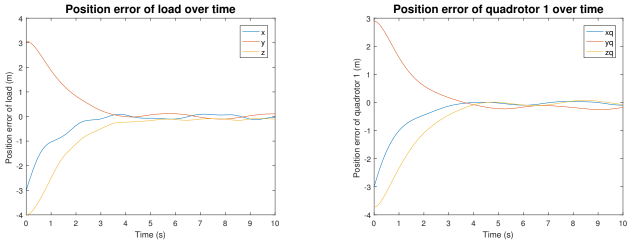

(a) Position error of load (b) Position error of quadrotor 1

Fig. 5. Simulation results for nonlinear model - circular trajectory with sinusoidal varying altitude - free flying

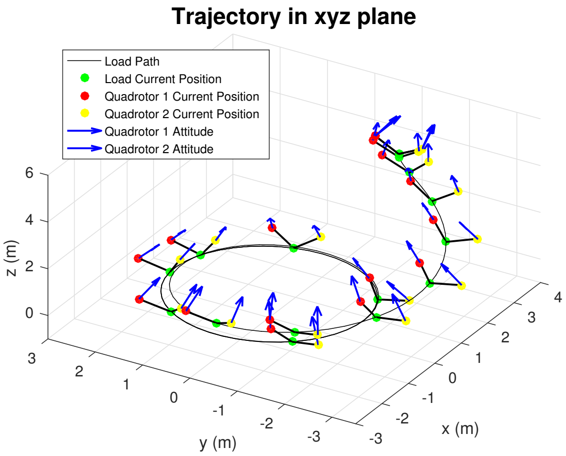

Fig. 6. Circular trajectory with fixed altitude

In Fig. 3, we can observe that the position error converges in approximately 10 seconds and the Lyapunov function reaches the value of 10^{-9} in 12 seconds, when the inner loop dynamics are neglected. With the inner loop controller, as observed in Fig. 4, the position error also converges to zero. However, the mean value reached by the Lyapunov function is about 10^{-4} instead of 10^{-9}. This is likely due to the derivative term approximation, as the angular velocity error states exhibit a sinusoidal-like variation due to the added delay in the derivative term. However the position error values still remain in low values, with a position error of about 0.0035 m.The 3-D trajectories of the load and quadrotors over time are shown in Fig. 6, where it is noticeable that the relative configuration of the cables remain approximately constant over time, as specified in the flat outputs. The position errors for the load and for one quadrotor are shown in Fig. 5. It can be observed that the free flying control solution does not adequately control the quadrotors to obtain the desired position, as the force interactions between the quadrotors and the load act as time-varying disturbances on the system. Neglecting these interactions causes an undamped solution, as observed in Fig. 5 b), which propagates to the position error of the load, as shown in Fig. 5 a). The mean error of the load for this solution is 0.1383 m - more than 4 times the mean value for the full model solution. These oscillations can also cause practical problems with the cable's ridigity assumptions not holding valid in an experiment, compromising the quadrotor and the load.

5. CONCLUSIONS

In this work, a novel control approach for trajectory tracking of a slung load using two quadrotors was proposed. The approach relies on the definition of a new set of flat outputs, which completely determine the relative configurations between the load and the quadrotors and have a simpler geometric interpretation than previously proposed outputs. For control system design an error system in cascaded form is incrementally constructed together with a cooperative control law for the two quadrotors that renders the origin of closed-loop system uniformly asymptotically stable. As demonstrated in the simulations in Section 4, the overall error state converges to zero, while maintaining the inputs within the physical limits of the actuators for each quadrotor.

REFERENCES

Cabecinhas, D., Cunha, R., and Silvestre, C. (2019). A trajectory tracking control law for a quadrotor with slung load. *Automatica*, 106, 384 – 389.

Kotaru, P., Wu, G., and Sreenath, K. (2017). Dynamics and control of a quadrotor with a payload suspended through an elastic cable. In *2017 American Control Conference (ACC)*, 3906–3913.

Lee, T. (2016). Optimal hybrid controls for global exponential tracking on the two-sphere. In *2016 IEEE 55th Conference on Decision and Control (CDC)*, 3331–3337.

Lee, T. (2018). Geometric control of quadrotor uavs transporting a cable-suspended rigid body. *IEEE Transactions on Control Systems Technology*, 26(1), 255–264.

Lee, T., Sreenath, K., and Kumar, V. (2013). Geometric control of cooperating multiple quadrotor uavs with a suspended payload. In *Proceedings of the IEEE Conference on Decision and Control*, 5510–5515.

Pereira, P.O. and Dimarogonas, D.V. (2017). Control framework for slung load transportation with two aerial vehicles. In *2017 IEEE 56th Annual Conference on Decision and Control (CDC)*, 4254–4259.

Pereira, P.O., Herzog, M., and Dimarogonas, D.V. (2016). Slung load transportation with a single aerial vehicle and disturbance removal. In *2016 24th Mediterranean Conference on Control and Automation (MED)*, 671–676.

Sreenath, K. and Kumar, V. (2013). Dynamics, Control and Planning for Cooperative Manipulation of Paylods Suspended by Cables from Multiple Quadrotor Robots. In *Robotics: Science and Systems 2013*.

Sreenath, K., Michael, N., and Kumar, V. (2013). Trajectory generation and control of a quadrotor with a cable-suspended load-A differentially-flat hybrid system. In *Proceedings of the 2013 IEEE International Conference on Robotics and Automation (ICRA)*, 4888–4895.

Villa, D.K.D., Brandão, A.S., and Sarcinelli-Filho, M. (2018). Load transportation using quadrotors: A survey of experimental results. In *2018 International Conference on Unmanned Aircraft Systems (ICUAS)*, 84–93.